



## Photodegradation of organic hazardous materials in presence of poly2-chloroaniline and poly 2-chloroaniline titanium dioxide quantum dots

Walied A. A. Mohamed<sup>1\*</sup>, Amr A. El Sammak<sup>2,3</sup>, Elsayed M. Elnaggar<sup>2,4</sup>, Badr A. El-Sayed<sup>2\*</sup>

<sup>1</sup>Photochemistry and Nanomaterials Lab, Department of Inorganic Chemistry, National Research Centre, Giza, Egypt.

<sup>2</sup>Department of Chemistry, Faculty of Science, Al-Azhar University, Nasr City, Cairo, Egypt.

<sup>3</sup>Chemicals Warfare Institute, Egypt Armed Forces, Egypt..



CrossMark

### Abstract

Conjugated polymers have recently been under active investigation as promising alternatives to use in photocatalysis. This is due to their unique advantages of low cost, high chemical stability, and molecularly tunable optoelectronic properties. This work explores the easy way to synthesize efficient poly2-chloroaniline (P2CIANI) via the chemical oxidative polymerization of P2CIANI. Titanium dioxide quantum dot (TiO<sub>2</sub> QD) have been prepared and used in preparation of P2CIANI/TiO<sub>2</sub> QD. X ray diffraction, FTIR, UV & Visible spectra, TGA, surface area, EDX and TEM measurements were used to characterize all prepared polymers. The photocatalytic activities of all recent polymers were investigated by the photo-degradation of methyl orange dye as an organic hazardous chemical in an aqueous medium was assessed using a 50-watt xenon lamp light source and direct sunlight. The effect of irradiation time, dye concentration and photo-catalyst amount on photo-degradation performance of the dye in presence of recent polymers were studied. P2CIANI/TiO<sub>2</sub> QD demonstrated high photocatalytic properties, with 80.3% efficiency, as opposed to 47% for P2CIANI only. When P2CIANI, TiO<sub>2</sub> QD, and P2CIANI/TiO<sub>2</sub> QD are present during the recycling processes in the presence of all created samples up to four times, the photo-degradation rate decreases by about 57.18, 9.61 and 9.51 % respectively.

**Keywords:** P2CIANI, P2CIANI/TiO<sub>2</sub> QD, Photocatalytic degradation, Methyl orange Dye.

### 1. Introduction

A polyaniline derivative called P2CIANI, has a chlorine (-Cl) group replaced in the ortho-position of the phenyl group [1–3]. P2CIANI, which features an electron-withdrawing chloro substituent, will undoubtedly result in a number of alterations to the polymer's characteristics [4–6]. Understanding the many characteristics of the polymeric material is crucial for using P2CIANI efficiently in possible applications, which is why there is increased interest in studying the polymer from various perspectives [7,8]. The most well-known oxidant for polymerizing polyaniline-based polymers is ammonium peroxydisulfate (APS) [9,10]. P2CIANI has good mechanical qualities, electrical conductivity, low cost, and environmental stability [11,12]. P2CIANI, one of the derivatives of polyaniline, exhibits superior solubility and processibility but has lower conductivity than PANI. However, among the protonated forms of P2CIANI, the emeraldine salt (ES; protonated form of emeraldine base EB) is the only one that conducts electricity [13]. Protonic acids or charge transfer with an oxidising agent can be used to dope PANI and its derivatives. By adjusting the doping level, its electrical and optical characteristics can be reversibly controlled [14,15]. P-type doping, which increases the number of holes

connected to the conjugated polymeric chain, is the doping method used in PANI and its variants. Positively charged holes are created as nitrogen atoms protonate, serving as the conjugated chain's charge carrier. PANI, undergoes a doping process that modifies its optical, morphological, and electrical properties [16,17].

Because of its stability, lack of toxicity, ease of production, broader band gap, and environmental friendliness, TiO<sub>2</sub> is a popular semiconductor photocatalyst. Numerous physical and chemical techniques can be used to further improve the photocatalytic activity of TiO<sub>2</sub> [18,19]. TiO<sub>2</sub> is a hydrophilic and photocatalytic metal oxide nanoparticle [20]. Due to their huge surface area and tremendous activity, quantum dots (QDs) have received a lot of interest. It has been discovered that QDs' physical and chemical characteristics differ from those of bulk materials [21,22]. To boost the photochemical activities and serve as a photocatalyst for the degradation of the methyl orange dye under visible and UV irradiation, TiO<sub>2</sub> QD was added to P2CIANI in this study [23,24].

### 2-Experimental section

#### 2-1-Materials

The following ingredients were purchased from Sigma Aldrich Co. 2-Chloroaniline (ortho-chloroaniline)

\*Corresponding author e-mail: [waliedfx@yahoo.com](mailto:waliedfx@yahoo.com); (Walied A. A. Mohamed).

Receive Date: 05 October 2023, Revise Date: 30 November 2023, Accept Date: 05 December 2023

DOI: 10.21608/EJCHEM.2023.240857.8712

©2024 National Information and Documentation Center (NIDOC)

monomer, concentrated hydrochloric acid (37%), ammonium persulfate [(NH<sub>4</sub>)<sub>2</sub>S<sub>2</sub>O<sub>8</sub>, APS], titanium tetrachloride, methanol annular, and methyl orang. 2-Chloroaniline was distilled under reduced pressure, and the other reagents were used without further processing.

## 2-2-Experimental methods

### 2-2-1-Preparation of P2CIANI

The template-free technique was employed to create P2CIANI. To decrease the amount of unpolymerized monomer and to increase the yield of P2CIANI, the oxidant's molar ratio was changed to 1.25 of the monomer ratios. By combining an aqueous solution with 1 mol of 2-chloroaniline and 1 mol of hydrochloric acid solution, P2CIANI hydrochloride monomer was created. To assure the creation of a homogeneous 2-chloroaniline-hydrochloride solution, the mixture was agitated for an hour. Deionized water was used to dissolve the pre-weighed APS before it was slowly added to the reaction mixture in a dropwise fashion while being vigorously stirred at room temperature for two hours. The mixture was then given 24 hours to polymerize. Gradually, the white colour of the solution turned to brown. The mixture is then filtered to produce the precipitate. To eliminate any contaminants, the precipitate was repeatedly rinsed with distilled water and a 0.5-molar hydrochloric acid solution before being allowed to dry at room temperature. In order to employ the P2CIANI powder in the characterization and evaluation processes, it was eventually gently ground and separated into parts[25,26].

### 2-2-2-Preparation of TiO<sub>2</sub> QD.

TiO<sub>2</sub> QD were made using a standard procedure that involved adding 20 mL of TiCl<sub>4</sub> gradually to 50 mL of methanol in an ice-water bath at 0 °C. Transparent to yellowish in colour, it was then put into a 100-mL Teflon-lined autoclave and heated to 90 °C for 24 hours. Centrifugation was used to get the final product, which was completely washed in methanol before being dried in the air at 70 °C for 24 hours[27,28].

### 2-2-3- Preparation of P2CIANI-TiO<sub>2</sub> QD.

To create P2CIANI/TiO<sub>2</sub> QD composites, in situ chemical polymerization was used. To ensure that TiO<sub>2</sub> QD was evenly distributed throughout the monomer solution, 10% by weight of 2-chloroaniline hydrochloride was taken as TiO<sub>2</sub> QD and suspended in the monomer solution using vigorous stirring for 30 minutes. The P2CIANI preparation method was employed to carry out the polymerization procedure.

### 2-2-4. Physical methods of measurements

Using a Philips diffractometer model X-ertpro (Netherlands), the crystallinity characteristics of P2CIANI, TiO<sub>2</sub>QD, and P2CIANI-TiO<sub>2</sub> QD samples were determined. The patterns were run with Ni-filtered copper radiation (CuK = 1.5404 Å at 10 mA and 30 kV with a scanning speed of 2 °/min). Thermo Scientific™ Talos F200i (STEM) is a 20–200 kV field emission (scanning) transmission electron microscope that was specifically

created for performance and productivity across a wide range of materials science samples and applications. It was used to study TiO<sub>2</sub> QDs and perform high-resolution 2D and 3D characterization, in situ dynamic observations, and diffraction applications. These included the kinetic slope ratio of fluorescence intensity to illumination time and the fluorescence rate constant (kf) of the item under inquiry. In addition, the absorbance spectra of the materials were examined in Japan using a UV260 model Shimadzu spectrometer. A UV-Vis-NIR spectrophotometer (Varian Cary 5E, USA) was used to measure the UV-Vis-NIR diffuse reflectance spectra of quantum dots at room temperature. These spectra were examined to determine the quantum dot's optical band gap. A photoreactor with a xenon lamp and a water-cooling mechanism was utilised to prevent the effect of lamp temperature on photo-degradation processes. To further examine the thermal behaviour, the PerkinElmer 4000, USA, thermal gravimetric analysis (TGA) was employed. Initial analysis temperatures of 30 °C to 900 °C to 1000 °C for PerkinElmer "Pyris" calibrations A mass flow controller is integrated, and the scanning speeds vary from 0.1 to 200 C/min. The temperature accuracy and precision are 1 and 0.8 degrees Celsius, respectively. TGA 4000 may be used to do thermogravimetric analysis (TGA) on both liquid and solid samples. It can measure mass as a function of temperature or time. Initial analysis temperatures of 30 °C to 900 °C to 1000 °C for PerkinElmer "Pyris" calibrations A mass flow controller is integrated, and the scanning speeds vary from 0.1 to 200 C/min. The temperature accuracy and precision are 1 and 0.8 degrees Celsius, respectively. TGA 4000 may be used to do thermogravimetric analysis (TGA) on both liquid and solid samples. It can measure mass as a function of temperature or time. These measurements offer details on chemical and physical processes, such as chemisorptions, thermal breakdowns, and solid-gas reactions (such as oxidation or reduction), as well as phase transitions, absorption, adsorption, and desorption. USA), sample preparation occurred by vacuum or flow techniques concomitant with sample analysis at different temperatures, and the gas surface area and micropore size analysis were utilised to identify the surface shape and microanalysis. 100 adsorption points and 100 desorption points formed the 200 data points used to analyse the sample. SEM model (Quanta FEG250, EDAX, FEI-inspects model), at 20–150 kV, magnifying an image at X 1.00 and X 100.000 by sending a beam of light through the object. energy dispersive X-ray (EDX) microanalysis. The Chemical Warfare Administration's laboratories employed a Bruker Spectrometer (model: ALPHAI WEEE-Reg DE84716930 - 24V; 3.0A, Germany) to take measurements in the 400–4000 cm<sup>-1</sup> range and record Fourier transform infrared (FT-IR) spectra. Egypt's Eng. Co., Ltd. initially constructed the system. The Xenon lamp provides light with a power density of 50 W/cm<sup>2</sup> and a wavelength range of 200–1100

nm. To avoid the heat lamp effect during photo-degradation processes, the gadget uses a water-cooling mechanism in conjunction with a 3 ml quartz cell for UV measurement. The photocatalytic activity was evaluated using a UV-VIS spectrophotometer, and diffuse reflectance spectra were collected using a UV-VIS-NIR spectrophotometer (VARIN CARY 5E, USA). In order to calculate the BET Specific Surface Area (BET SSA), a Perkin Elmer Lambda 35 was employed. USA, Quantachrome, Nova3000e The samples were examined in a nitrogen-based environment (77 K adsorption-desorption isotherms). Before the investigation, the materials were dried for an hour at 150 degrees Celsius. The Barrett, Joyner, and Halenda methods can be used to calculate the average pore size and pore size distribution[29,30].

### 2-3-Photocatalytic activity

We assessed the photocatalytic activity of P2CIANI / TiO<sub>2</sub> QDs used as photocatalysts for photo-degradation in dyeing processes utilising xenon photo-reactors and direct solar radiation. A 50-watt Xenon lamp with a wavelength range of 200–1100 nm was used in the experimental setup for the photocatalytic investigation (Eng. Co., Ltd., Egypt). As a model for commercial dyes, the photo-degradation of the dye methyl orange was used to evaluate photocatalytic activity. Under test circumstances with a pH of 6.9, 0.25 mg from the created samples were added to 500 ml of methyl orange dye (2 x10<sup>-5</sup> M). The tested mixture was then centrifuged for 20 minutes at 10,000 rpm. The photodegradation rates of all processed samples are represented by the following equation:

$$\ln C_0 / C = k_{\text{app}} t \quad (1)$$

where C<sub>0</sub> represents the dye concentration at the beginning, C represents the dye concentration at time t, and k<sub>app</sub> represents the photodegradation process' rate constant. By incorporating TD's catalyst into the dye solution and then stirring it in the dark for 20 minutes, the adsorption and desorption processes could be balanced. When xenon was present, the photodegradation process was stopped (at 50 watts). After 180 minutes of exposure, used samples of PANI and PANI/TiO<sub>2</sub> QDs photocatalysts were examined, including recycling. The utilised PANI and PANI/TiO<sub>2</sub> QDs samples were thoroughly cleaned with deionized water, centrifuged at a speed of 14000 rpm, and then dried for twenty-four hours at 80° C. After drying under the same experimental conditions as before, the same quantity of the recovered P2CIANI and P2CIANI-TiO<sub>2</sub>QDs was used once more, and the decolorization (%) was measured using Eq. (1) [31,32].

Important characteristics of the organic matter include their ability to: form water-soluble and water insoluble complexes with metal ions and hydrous oxides, introduced organic compounds; absorb and release plant nutrients; and hold water in the soil environment. As a result of these characteristics, the determination of total organic carbon (a measure of one of the chemical components of organic matter that is often used as an indicator of its presence in a

soil or sediment) is an essential part of any site characterization since its presence or absence can markedly influence how chemicals will react in the soil or sediment. Soil and sediment total organic carbon (TOC), TOC contents may be used qualitatively to assess the nature of the sampling location (e.g., was a depositional area) or may be used to normalize portions of the analytical chemistry data set Two general approaches are used to measure TOC. One approach determines TOC by subtracting the measured total inorganic carbon value (TIC) from the measured total carbon value (TC), which is the sum of organic carbon and inorganic carbon[33,34].

$$\text{TOC} = \text{TC} - \text{TIC}$$

The other approach first purges the TIC from the sample before any organic carbon measurement is performed. However, this TIC purging step also purges some organic molecules (purgeable organic substance, such as benzene, toluene, cyclohexane and chloroform may partly escape on stripping), which can be re trapped and oxidised to CO<sub>2</sub>.

## 3. Results and Discussion

### 3-1- XRD analysis.

Figure (1) depicts the XRD pattern of synthesised P2CIANI, TiO<sub>2</sub> QD, and P2CIANI/TiO<sub>2</sub> QD. The characteristic peak of the pure P2CIANI powders is seen by the XRD of P2CIANI at  $2\theta = 26^\circ$ . The polyaniline family is characterised by this peak, which is sharper in polyaniline. It suggests some degree of polymer crystallisation. P2CIANI has an amorphous form, as demonstrated by[35–37]. TiO<sub>2</sub>QD's great crystallinity is revealed by the XRD, which exhibits a very sharp peak at 25.3° and smaller peaks centred at  $2\theta = 38.1^\circ, 48.^\circ, 55.2^\circ, 62^\circ, 69.1^\circ,$  and  $75.5^\circ$ [38,39]. The pattern of P2CIANI/TiO<sub>2</sub>QD nanocomposites mainly indicates the presence of TiO<sub>2</sub> characteristic peaks shown at  $2\theta = 25.5^\circ, 38.07^\circ, 48.13^\circ, 55^\circ, 61.8^\circ,$  and  $75.5^\circ$  in addition to characteristic peaks of P2CIANI at  $2\theta = 26^\circ$  that are assigned to periodicity parallel and perpendicular to the chain direction of P2CIANI, while the peak at 25.3° is overlapped and These peaks are referred to JCPDS-ICDD file No. 84-1285.

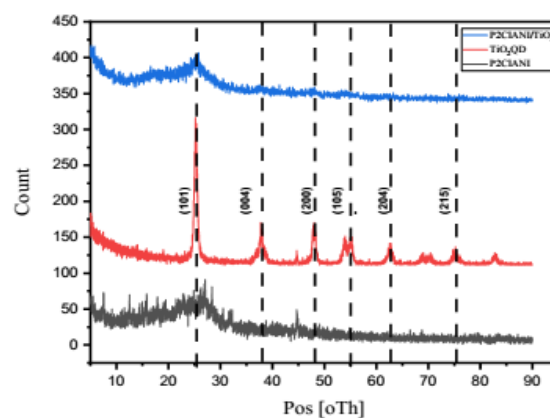


Figure (1) X-Ray Diffraction Studies of patterns of (P2CIANI-TiO<sub>2</sub>QD-P2CIANI/TiO<sub>2</sub>QD).

### 3-2- TEM analysis.

The TEM pictures of the P2CIANI polymer are shown in Figure (2). The TEM image clearly shows that P2CIANI, which has a diameter of 30 to 40 nm and denotes large globular agglomerates with a smooth surface, was synthesised as a nanoparticle[40–42]. Due to the TiO<sub>2</sub> (quantum dot)'s small nanoparticle size, the conformal TiO<sub>2</sub> layer's thickness can be seen in the TEM picture of the TiO<sub>2</sub> QD to be approximately 3-5 nm[43]. Additionally, TEM images of the P2CIANI/TiO<sub>2</sub> QD show that TiO<sub>2</sub> QD and P2CIANI sequentially create connections in the nanocomposite. The TEM photos also demonstrated that TiO<sub>2</sub> QD is entirely integrated in the polymer matrix, and the nanocomposite grew more compact. Although at a small concentration of nanoparticles, TiO<sub>2</sub> QD also uniformly diffused in the polymer and demonstrated the gritty morphology common to all polymer nanocomposites.

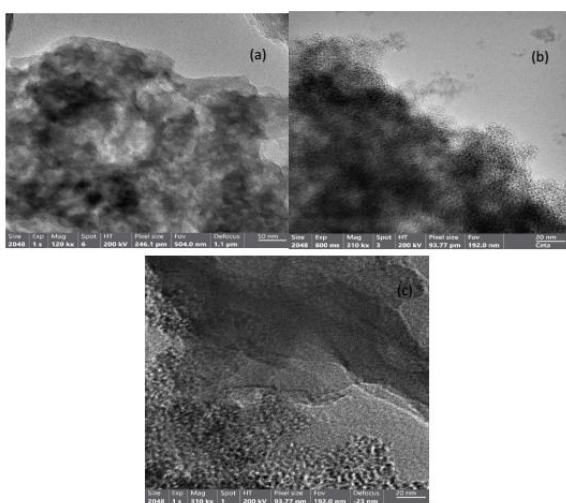


Figure (2) TEM image for P2CIANI (a), TiO<sub>2</sub> QD (b) and P2CIANI/TiO<sub>2</sub> QD (c).

### 3-3- EDX analysis.

The EDX spectrum contains both quantitative and qualitative data. Since air molecules are strong X-ray and electron absorbers, it is evident that this has an effect on the prepared samples since all created samples are evaluated in a vacuum. The results demonstrate that the elements in composites, namely nitrogen, carbon, sulphur, oxygen, and chlorine, show distinguishable X-ray elemental maps in Figure 3a of P2CIANI, while C and N are the skeleton of P2CIANI. Figure (3)c illustrates the previously mentioned elements in P2CIANI (carbon, oxygen, sulphur, and chlorine), in addition to the titanium element, and this confirms the association of the titanium element with the primary components of P2CIANI in the matrix structure of the composite. Fig. 3 b also explains the structural composition of the element titanium dioxide.

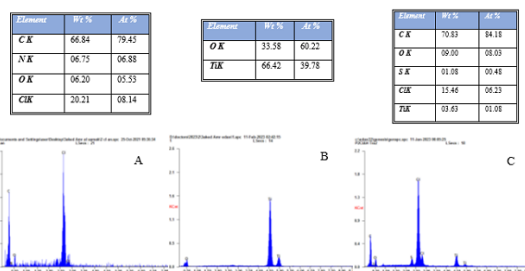


Figure (3) EDX of P2CIANI, TiO<sub>2</sub> QD and P2CIANI/TiO<sub>2</sub> QD

### 3-4- FTIR Analysis

Fig. 4a displays the FTIR spectra of pure P2CIANI. At 3339 cm<sup>-1</sup>, the peak of the NH-asymmetric stretching vibrations can be found. The aromatic C=C asymmetric stretching vibrations of the quinonoid and benzene rings, respectively, are what cause the 1571 and 1492 cm<sup>-1</sup> bands. At 1290 cm<sup>-1</sup>, the aromatic C-N stretching vibrations are visible. The (C-C) asymmetric stretching in plane C-H bending modes, respectively, is what causes the bands at 1162 cm<sup>-1</sup>. The C-H out of plane bending is represented by the bands at 907 and 827 cm<sup>-1</sup>. 1,2,4-trisubstituted aromatic ring's asymmetric stretching vibration. All the benzene rings stated above support the peak at 811 cm<sup>-1</sup>, which is the chloro group connected to the P2CIANI structure. band features at 668 cm<sup>-1</sup> in[44–46] the FTIR of the TiO<sub>2</sub> QD spectra are attributed to the Ti-O-Ti bonds and O-H stretching vibration at 3419 cm[47,48]. Additionally, the FTIR of P2CIANI/TiO<sub>2</sub>QD was seen in Figure 4C, which shows the FTIR of the P2CIANI/TiO<sub>2</sub>QD nanocomposite spectrum. This confirms the chemical structure of the generated nanocomposite as recommended. The nanocomposite's distinctive mane is classified as a flow. The hydrogen-linked N-H between the amin and imine sites, which has a minor shift from pure P2CIANI due to TiO<sub>2</sub>, is responsible for the absorption peak detected at 3223 cm<sup>-1</sup>. The quinoid and benzenoid units' respective C=N and C=C asymmetric stretching modes are responsible for the absorption pecks seen at 1569 and 1497 cm<sup>-1</sup>. The strong band at 1185 cm<sup>-1</sup> measures the degree of electron delocalization and is hence the distinctive peak of P2CIANI conductivity. The band at 1289 cm<sup>-1</sup> is attributed to the C-N stretching vibration mode of the benzenoid unit. As a transition metal, titanium has a strong propensity to combine with the nitrogen atom in the P2CIANI macromolecule to generate coordination compounds. The C=N, C=C, and C-N bond strengths in the P2CIANI macromolecule may be weakened by this interaction. These findings attest to the presence of P2CIANI in the TiO<sub>2</sub> QD nanocomposite. It is clear that the concentration of TiO<sub>2</sub> boosted this peak's strength. This fact might imply that doping TiO<sub>2</sub> can effectively facilitate electron delocalization.

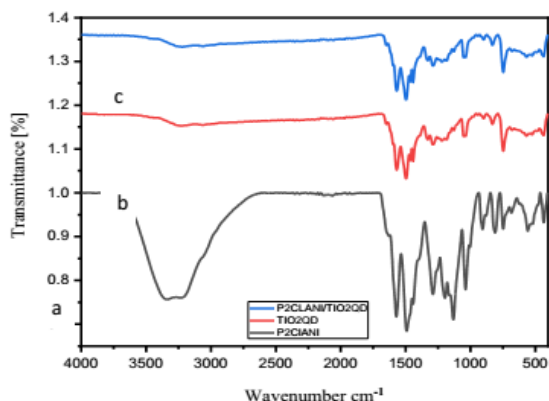


Figure (4) FTIR of P2CIANI-TiO<sub>2</sub>QD-P2CIANI/TiO<sub>2</sub>QD

3-5- UV-vis diffuse reflectance (UV-vis-DR) spectra  
The optical band gap energy ( $E_g$ ) close to the band edge and the absorption coefficient have the following relationship:

$$\alpha h\nu = A (h\nu - E_g)^{1/2}$$

where the photon energy and a constant, respectively, are denoted by  $h\nu$  and  $A$ . Extrapolating the linear component of the curve  $(\alpha h\nu)^2$  to  $h\nu$  will yield the band of P2CIANIs. For P2CIANI, the predicted band gaps are 3.89, 2.25 and 2.42. The band gap narrows as the oxidation state rises, which is in good agreement with earlier findings. This phenomenon matches the PANIs' colour change as well[49].

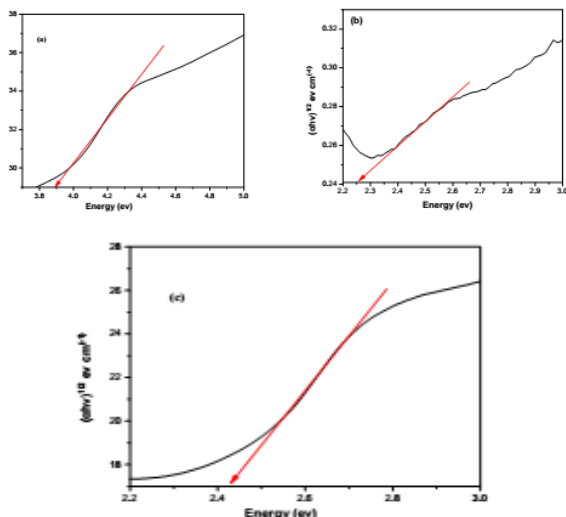


Figure (5) UV-vis diffuse reflectance (UV-vis-DR) spectra of P2CIANI-EcS,

### 3-6 - TGA analysis.

Figure (6 a) displays the TGA curves created for P2CIANI, where "residual wt.%" stands for the substance's weight percentage content. P2CIANI's thermal behaviour typically loses weight in four stages. The initial stage of weight loss occurs around 100°C due to water loss, with a loss percentage of roughly 5%. The removal of HCL caused the

second weight loss below 300°C, when the loss percentage was around 20%. The third weight loss decomposition temperature takes place between 300 and 464°C; once the dopant acids are removed from the structure, the polymer chain structure decomposes, and the exothermic decomposition of P2CIANI begins at around 500°C, where the loss percentage was around 35%. The fourth and final phase was the breakdown of P2CIANI, which continued up to 700°C and continued even after that point in time. Some character content is left over from the P2CIANI's breakdown. This demonstrates that chlorine, where the loss percentage was about 55% [50–52], has prevented full breakdown. Figure (6 b) depicts the TGA of TiO<sub>2</sub> QD. This demonstrates titanium's resistance to heat up to 900°C due to the element's nature as an inorganic metal oxide [53]. Figure (6 c) depicts a TGA P2CIANI/TiO<sub>2</sub> QD composite, demonstrating the stability of P2CIANI after being doped

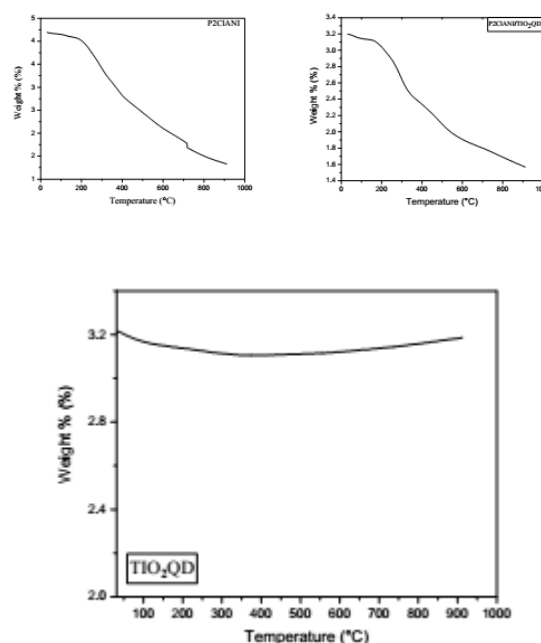


Figure (6) TGA of P2CIANI, TiO<sub>2</sub>QD and P2CIANI-TiO<sub>2</sub>QD

The polymer chain structure is destroyed after the dopant acids are removed from the structure, and the exothermic decomposition of P2CIANI begins around 500°C, where the loss percentage is about 35% and the composite thermal resistance increases to 500°C. This is the third weight-loss decomposition temperature. The fourth and last stage involves constant P2CIANI breakdown between 700 and 900°C degrees Celsius. The entire breakdown has not yet occurred, even at 700°C. It shows that titanium quantum dot doping has increased the thermal stability of P2CIANI/TiO<sub>2</sub> QD over pure P2CIANI and reduced the loss percentage to 50% from 55% for pure P2CIANI.

### 3.7. Photocatalytic activity

The first-order kinetics follows photocatalytic studies with Methyl orange Dye and the correlation between maximum photodegradation percentage, photodegradation times, and

photodegradation rates of the prepared samples represented in fig. 7. The findings showed that photodegradation rates increases as in P2CIANI/TiO<sub>2</sub>QD than P2CIANI because of presence of TiO<sub>2</sub> QD which due to the photocatalytic activity of TiO<sub>2</sub>QD supported on P2CIANI which increase the active site during the photodegradation process[54–56].

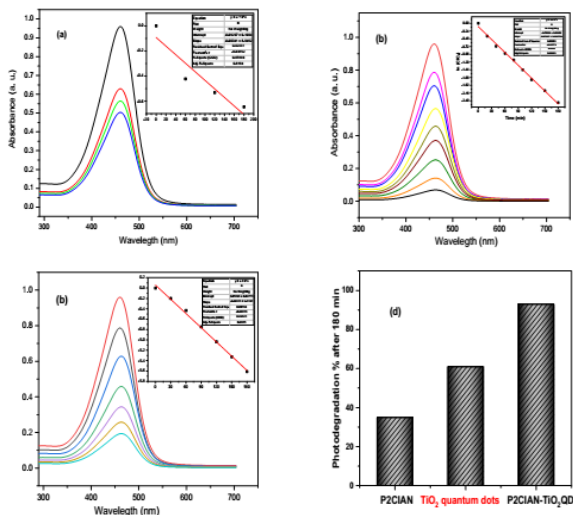
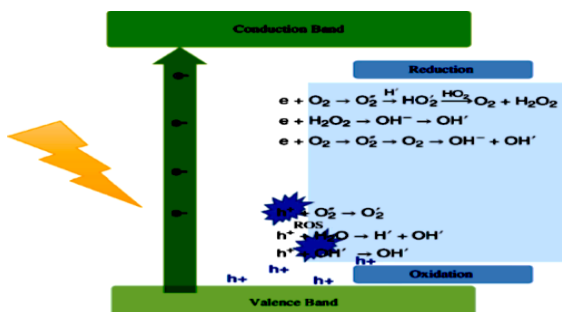
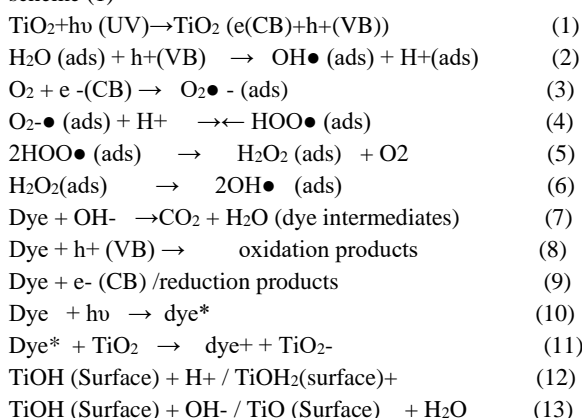


Figure 7. P2CIANI (a), (b) TiO<sub>2</sub>QD, P2CIANI/TiO<sub>2</sub>QD (c) and photodegradation % after 180 min (d).

The suggested degradation mechanism for the photodegradation process as the following equation and scheme (1)



Scheme 1. Suggested photodegradation mechanism in presence of titanium dioxide quantum dots

Recently, conducting polymer especially P2CIANI shows great potential as photosensitizer due to its particular features such as low band gap and  $\pi$ - $\pi^*$  transition which the electron can be excited from highest occupied molecular orbital (HOMO) to lowest unoccupied molecular orbital (LUMO)[57]. In fact, P2CIANI had attracted many attentions by its special properties such as high conductivity, good environmental stability, cheap monomer, and ease of preparation. Doping of P2CIANI with TiO<sub>2</sub> QD has lowered its band gap and shifts optical response to visible light region[58]. The photodegradation rate for P2CIANI-TiO<sub>2</sub>QD is  $(9.15 \times 10^{-3})$  and higher than P2CIANI  $(3.41 \times 10^{-3})$  while it is  $(13.31 \times 10^{-3})$  for TiO<sub>2</sub> QD because of presence of TiO<sub>2</sub> QD which due to the photocatalytic activity of TiO<sub>2</sub> QD supported on P2CIANI which increase the active site as an active photocatalyst during the photodegradation process on the aniline ring beside the chloronyl active negative group attached to aniline ring which enhances the oxidation-reduction reaction on the photocatalyst surface due to this distinguishable increase (triple time) in the photodegradation rate in P2CIANI-TiO<sub>2</sub>QD than P2CIANI. Also, photodegradation percentages after irradiation by xenon lamp (50 Watt) for 180 min indicate that the photocatalytic activity for P2CIANI /TiO<sub>2</sub>QD recorded high photodegradation percentage (80.03%) higher than P2CIANI which recorded (47%). This observation refers to effect of the photocatalytic activity of TiO<sub>2</sub>QD which increase the photodegradation percentage by nearly about 70.2 % in case of using P2CIANI /TiO<sub>2</sub>QD compared to pure P2CIANI[59,60].

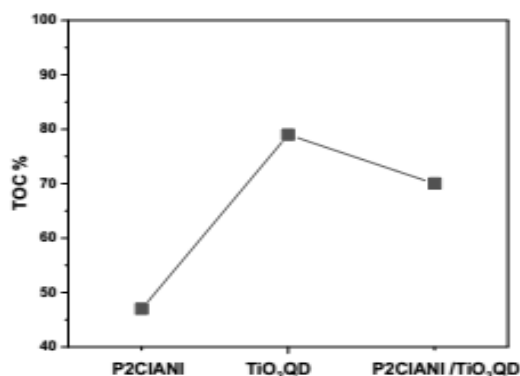


Figure 8. TOC % of photodegradation of Methyl Orange dye in different catalysts.

TOC test forces the analytical technology toward instruments able to ensure a complete oxidation (mineralisation to CO<sub>2</sub>) of all the possible organic compounds, Water matrices surely contain also inorganic carbon (dissolved CO<sub>2</sub>, carbonate and bicarbonate), so all methods must discriminate between the inorganic carbon and CO<sub>2</sub> produced from the oxidation of organic molecules in the sample as shown in figure (8) where the TOC percentages of (PCI-AN), TQD, and (PCI-AN)/TQD recorded 46%, 70%, and 79% respectively, and similar to

the photodegradation % obtained from photodegradation processes of Methyl Orange Dye.

### 3.8. Recycling process

Figure (9) shows that the rate of photodegradation processes reduces during the process of recycling in presence of all prepared samples till 5 times for across all photodegradation processes. The variation in the rates of photodegradation processes between all prepared samples have distinguishable observation where the photodegradation rate decreases by nearly about 57.18, 9.61 and 9.51 % in presence of P2CIANI, TiO<sub>2</sub> QD and P2CIANI/ TiO<sub>2</sub>QD, respectively as shown in Figure 10. Also, it can be concluded that during the photodegradation processes using xenon irradiation source, the presence of TiO<sub>2</sub> QD in the recycling processes times have small effect on the photodegradation process due to the small decreasing in the photodegradation rates observed and let a chance for the prepared catalyst to recycling for five times[61–63].

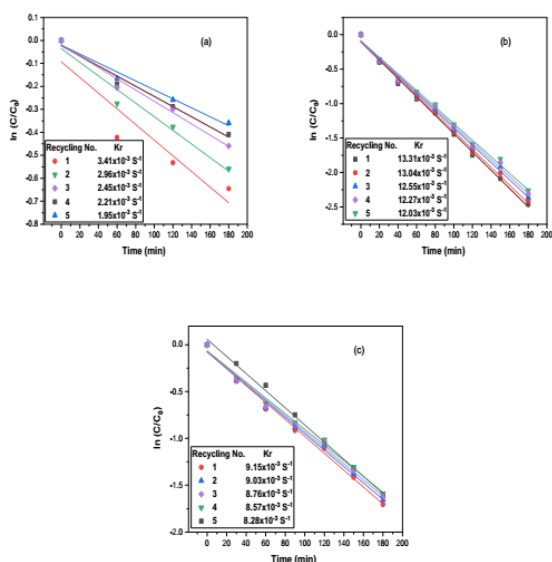


Figure 9. Kinetics plot for recycling process of photodegradation process of Methyl orange Dye in the presence of P2CIANI(a), TiO<sub>2</sub> QD(b), P2CIANI-TiO<sub>2</sub> QD (c).

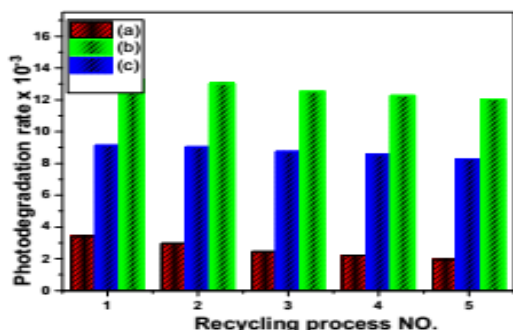


Figure 10. Photodegradation rates of Methyl orange Dye in the presence of P2CIANI(a), TiO<sub>2</sub> QD(b), P2CIANI-TiO<sub>2</sub> QD using Xenon photoreactor.

### Conclusion.

In this study, P2CIANI and TiO<sub>2</sub> QD with oxidants (APS) were immediately converted into new nanocomposites using the chemical oxidation polymerization method. According to the findings of FTIR, EDX, and UV-vis-DR visible diffuse reflectance spectra measurements, the nanocomposites, which included both P2CIANI and TiO<sub>2</sub>QD, were successfully synthesised. In fact, TEM images show that the P2CIANI shell has an average total diameter of 35–40 nm and surrounds the TiO<sub>2</sub>QD particle core. P2CIANI degrades into a low-crystalline or amorphous structure, according to XRD studies, but TiO<sub>2</sub>QD is crystalline, increasing crystallinity when compared to P2CIANI. Adding TiO<sub>2</sub> QD to the P2CIANI/TiO<sub>2</sub>QD composite boosts P2CIANI stability at high temperatures, according to TGA testing. In the end, introducing TiO<sub>2</sub>QD to P2CIANI/TiO<sub>2</sub>QD around % increased the photocatalytic activity of P2CIANI's efficiency. The photo-degradation rate lowers by about 17.4, 15.4, and 50.2% in the presence of P2CIANI/TiO<sub>2</sub> QD, titanium dioxide quantum dots, and P2CIANI, respectively, in four recycling procedures when all produced catalysts are present.

### References

- [1] M.N. Ahmad, F. Rafique, F. Nawaz, T. Farooq, M.N. Anjum, T. Hussain, S. Hassan, M. Batool, H. Khalid, K. Shehzad, Synthesis of antibacterial poly(o-chloroaniline)/chromium hybrid composites with enhanced electrical conductivity, *Chem Cent J.* 12 (2018). <https://doi.org/10.1186/s13065-018-0416-3>.
- [2] T. Hussain, M.N. Ahmad, A. Nawaz, A. Mujahid, F. Bashir, G. Mustafa, Surfactant incorporated co nanoparticles polymer composites with uniform dispersion and double percolation, *J Chem.* 2017 (2017). <https://doi.org/10.1155/2017/7191590>.
- [3] P. Zhang, R.Y. Hong, Q. Chen, W.G. Feng, On the electrical conductivity and photocatalytic activity of aluminum-doped zinc oxide, *Powder Technol.* 253 (2014) 360–367. <https://doi.org/10.1016/j.powtec.2013.12.001>.
- [4] Z. Zhang, Z. Wei, M. Wan, Nanostructures of polyaniline doped with inorganic acids, *Macromolecules.* 35 (2002) 5937–5942. <https://doi.org/10.1021/ma020199v>.
- [5] Y. Jafari, M. Shabani-Nooshabadi, S.M. Ghoreishi, Poly(2-chloroaniline) electropolymerization coatings on aluminum alloy 3105 and evaluating their corrosion protection performance, *Transactions of the Indian Institute of Metals.* 67 (2014) 511–520. <https://doi.org/10.1007/s12666-013-0374-3>.
- [6] B.T. Raut, M.A. Chougule, A.A. Ghanwat, R.C. Pawar, C.S. Lee, V.B. Patil, Polyaniline-CdS nanocomposites: Effect of camphor sulfonic acid

- doping on structural, microstructural, optical and electrical properties, *Journal of Materials Science: Materials in Electronics*. 23 (2012) 2104–2109. <https://doi.org/10.1007/s10854-012-0708-7>.
- [7] S.S. Pandule, S.U. Shisodia, M.R. Patil, R.P. Pawar, V. V. Chabukswar, Synthesis and characterization of methanesulfonic acid doped poly(2-chloroaniline), study of its physical properties and ammonia gas sensing application, *Journal of Macromolecular Science, Part A: Pure and Applied Chemistry*. 53 (2016) 768–772. <https://doi.org/10.1080/10601325.2016.1237815>.
- [8] Z. Hu, M. Wang, S. Li, X. Liu, J. Wu, Ortho alkyl substituents effect on solubility and thermal properties of fluorenyl cardo polyimides, *Polymer (Guildf)*. 46 (2005) 5278–5283. <https://doi.org/10.1016/j.polymer.2005.04.060>.
- [9] P. Kong, P. Liu, Z. Ge, H. Tan, L. Pei, J. Wang, P. Zhu, X. Gu, Z. Zheng, Z. Li, Conjugated HCl-doped polyaniline for photocatalytic oxidative coupling of amines under visible light, *Catal Sci Technol*. 9 (2019) 753–761. <https://doi.org/10.1039/c8cy02280a>.
- [10] M. Ando, C. Swart, E. Pringsheim, V.M. Mirsky, O.S. Wolfbeis, Optical ozone-sensing properties of poly(2-chloroaniline), poly(N-methylaniline) and polyaniline films, in: *Sens Actuators B Chem*, 2005: pp. 528–534. <https://doi.org/10.1016/j.snb.2004.12.083>.
- [11] A. Ays, egü L Gö, B. Sari, M. Talu, Chemical Preparation of Conducting Polyfuran/Poly(2-chloroaniline) Composites and Their Properties: A Comparison of Their Components, *Polyfuran and Poly(2-chloroaniline)*, 2003.
- [12] L.I. Dan, J. Huang, R.B. Kaner, Polyaniline nanofibers: a unique polymer nanostructure for versatile applications, *Acc Chem Res*. 42 (2009) 135–145. <https://doi.org/10.1021/ar800080n>.
- [13] A. Gök, S. Şen, Preparation and characterization of poly(2-chloroaniline)/SiO<sub>2</sub> nanocomposite via oxidative polymerization: Comparative UV-vis studies into different solvents of poly(2-chloroaniline) and poly(2-chloroaniline)/SiO<sub>2</sub>, *J Appl Polym Sci*. 102 (2006) 935–943. <https://doi.org/10.1002/app.24266>.
- [14] A.G. Macdiarmid, A.J. Epstein, Secondary doping in polyaniline, 1995.
- [15] A.K. Cuentas-Gallegos, M. Lira-Cantú, N. Casañ-Pastor, P. Gómez-Romero, Nanocomposite hybrid molecular materials for application in solid-state electrochemical supercapacitors, *Adv Funct Mater*. 15 (2005) 1125–1133. <https://doi.org/10.1002/adfm.200400326>.
- [16] W. Kongkaew, W. Sangwan, W. Prissanaroon-Ouajai, A. Sirivat, Synthesis and characterization of poly(2-chloroaniline) by chemical oxidative polymerization, *Chemical Papers*. 72 (2018) 1007–1020. <https://doi.org/10.1007/s11696-017-0343-0>.
- [17] Z. Hu, M. Wang, S. Li, X. Liu, J. Wu, Ortho alkyl substituents effect on solubility and thermal properties of fluorenyl cardo polyimides, *Polymer (Guildf)*. 46 (2005) 5278–5283. <https://doi.org/10.1016/j.polymer.2005.04.060>.
- [18] M.M. Khan, S.A. Ansari, D. Pradhan, M.O. Ansari, D.H. Han, J. Lee, M.H. Cho, Band gap engineered TiO<sub>2</sub> nanoparticles for visible light induced photoelectrochemical and photocatalytic studies, *J Mater Chem A Mater*. 2 (2014) 637–644. <https://doi.org/10.1039/c3ta14052k>.
- [19] S. Kalathil, M.M. Khan, S.A. Ansari, J. Lee, M.H. Cho, Band gap narrowing of titanium dioxide (TiO<sub>2</sub>) nanocrystals by electrochemically active biofilms and their visible light activity, *Nanoscale*. 5 (2013) 6323–6326. <https://doi.org/10.1039/c3nr01280h>.
- [20] W.A.A. Mohamed, A. Fahmy, A. Helal, E.A.E. Ahmed, B.A. Elsayed, E.A. Kamoun, E.A.M. Gad, Degradation of local Brilliant Blue R dye in presence of polyvinylidene fluoride/MWCNs/TiO<sub>2</sub> as photocatalysts and plasma discharge, *J Environ Chem Eng*. 10 (2022). <https://doi.org/10.1016/j.jece.2021.106854>.
- [21] L. Gnanasekaran, R. Hemamalini, K. Ravichandran, Synthesis and characterization of TiO<sub>2</sub> quantum dots for photocatalytic application, *Journal of Saudi Chemical Society*. 19 (2015) 589–594. <https://doi.org/10.1016/j.jscs.2015.05.002>.
- [22] R. Danish, F. Ahmed, B.H. Koo, Rapid synthesis of high surface area anatase Titanium Oxide quantum dots, *Ceram Int*. 40 (2014) 12675–12680. <https://doi.org/10.1016/j.ceramint.2014.04.115>.
- [23] L. Zhu, W.J. An, J.W. Springer, L.B. Modesto-Lopez, S. Gullapalli, D. Holten, M.S. Wong, P. Biswas, Linker-free quantum dot sensitized TiO<sub>2</sub> photoelectrochemical cells, *Int J Hydrogen Energy*. 37 (2012) 6422–6430. <https://doi.org/10.1016/j.ijhydene.2012.01.028>.
- [24] M. Ando, C. Swart, E. Pringsheim, V.M. Mirsky, O.S. Wolfbeis, Optical ozone-sensing properties of poly(2-chloroaniline), poly(N-methylaniline) and polyaniline films, in: *Sens Actuators B Chem*, 2005: pp. 528–534. <https://doi.org/10.1016/j.snb.2004.12.083>.
- [25] E.M. Elnaggar, K.I. Kabel, A.A. Farag, A.G. Al-Gamal, Comparative study on doping of polyaniline with graphene and multi-walled carbon nanotubes, *J Nanostructure Chem*. 7 (2017) 75–83. <https://doi.org/10.1007/s40097-017-0217-6>.
- [26] W. Kongkaew, W. Sangwan, W. Prissanaroon-Ouajai, A. Sirivat, Synthesis and characterization of poly(2-chloroaniline) by chemical oxidative polymerization, *Chemical Papers*. 72 (2018) 1007–1020. <https://doi.org/10.1007/s11696-017-0343-0>.
- [27] W.A.A. Mohamed, H.H. Abd El-Gawad, H.T. Handal, H.R. Galal, H.A. Mousa, B.A. Elsayed, A.A. Labib, M.S.A. Abdel-Mottaleb, TiO<sub>2</sub> quantum dots: Energy

- consumption cost, germination, and phytotoxicity studies, recycling photo and solar catalytic processes of reactive yellow 145 dye and natural industrial wastewater, *Advanced Powder Technology*. 34 (2023). <https://doi.org/10.1016/j.apt.2022.103923>.
- [28] M.R. Al-Mamun, S. Kader, M.S. Islam, M.Z.H. Khan, Photocatalytic activity improvement and application of UV-TiO<sub>2</sub> photocatalysis in textile wastewater treatment: A review, *J Environ Chem Eng*. 7 (2019). <https://doi.org/10.1016/j.jece.2019.103248>.
- [29] L. Huang, X. Zhuang, J. Hu, L. Lang, P. Zhang, Y. Wang, X. Chen, Y. Wei, X. Jing, Synthesis of biodegradable and electroactive multiblock polylactide and aniline pentamer copolymer for tissue engineering applications, *Biomacromolecules*. 9 (2008) 850–858. <https://doi.org/10.1021/bm7011828>.
- [30] Y.-C. Liu, C.-J. Tsai, Characterization and enhancement in conductivity and conductivity stability of electropolymerized polypyrrole/Al<sub>2</sub>O<sub>3</sub> nanocomposites, n.d. [www.elsevier.com/locate/jelechem](http://www.elsevier.com/locate/jelechem).
- [31] R. Gailliot-Vuillecot, A.L. Thomann, T. Lecas, C. Cachoncinlle, E. Millon, A. Caillard, Hot target magnetron sputtering process: Effect of infrared radiation on the deposition of titanium and titanium oxide thin films, *Vacuum*. 181 (2020). <https://doi.org/10.1016/j.vacuum.2020.109734>.
- [32] M. Rahiminezhad–Soltani, K. Saberyan, A. Simchi, New insight into reaction mechanisms of TiCl<sub>4</sub> for the synthesis of TiO<sub>2</sub> nanoparticles in H<sub>2</sub>O-assisted atmospheric-pressure CVS process, *Mater Sci Eng B Solid State Mater Adv Technol*. 264 (2021). <https://doi.org/10.1016/j.mseb.2020.114958>.
- [33] B.A. Schumacher, METHODS FOR THE DETERMINATION OF TOTAL ORGANIC CARBON (TOC) IN SOILS AND SEDIMENTS, 2002.
- [34] G. Visco, L. Campanella, V. Nobili, Organic carbons and TOC in waters: An overview of the international norm for its measurements, in: *Microchemical Journal*, 2005: pp. 185–191. <https://doi.org/10.1016/j.microc.2004.10.018>.
- [35] P. Lingnathan, M. Samuel, Effect of Dodecyl Benzene Sulphonic Acid on the Electrical Conductivity Behaviour of Poly(2-chloroaniline) and Poly(2-chloroaniline)/Silk Blends, *American Journal of Polymer Science*. 2014 (2014) 107–116. <https://doi.org/10.5923/j.ajps.20140404.02>.
- [36] O.A. Anunziata, M.B. Gómez Costa, R.D. Sánchez, Preparation and characterization of polyaniline-containing Na-*Al*MCM-41 as composite material with semiconductor behavior, *J Colloid Interface Sci*. 292 (2005) 509–516. <https://doi.org/10.1016/j.jcis.2005.06.002>.
- [37] A. Maity, M. Biswas, A Nanocomposite of Poly(N-vinylcarbazole) with Nanodimensional Alumina, 2003.
- [38] E.P. Ferreira-Neto, M.A. Worsley, U.P. Rodrigues-Filho, Towards thermally stable aerogel photocatalysts: TiCl<sub>4</sub>-based sol-gel routes for the design of nanostructured silica-titania aerogel with high photocatalytic activity and outstanding thermal stability, *J Environ Chem Eng*. 7 (2019). <https://doi.org/10.1016/j.jece.2019.103425>.
- [39] M. Rahiminezhad–Soltani, K. Saberyan, A. Simchi, New insight into reaction mechanisms of TiCl<sub>4</sub> for the synthesis of TiO<sub>2</sub> nanoparticles in H<sub>2</sub>O-assisted atmospheric-pressure CVS process, *Materials Science and Engineering: B*. 264 (2021). <https://doi.org/10.1016/j.mseb.2020.114958>.
- [40] S. Saikrithika, S.T. Huang, A. Senthil Kumar, Electrochemical polymerization of para-chloroaniline as highly redox-active poly(para-chloroaniline) on graphitized mesoporous carbon surface, *Electrochim Acta*. 349 (2020). <https://doi.org/10.1016/j.electacta.2020.136376>.
- [41] W. Kongkaew, W. Sangwan, W. Prissanaroon-Oujai, A. Sirivat, Synthesis and characterization of poly(2-chloroaniline) by chemical oxidative polymerization, *Chemical Papers*. 72 (2018) 1007–1020. <https://doi.org/10.1007/s11696-017-0343-0>.
- [42] H.W. Ki, H.C. Min, M.K. Chong, M. Xu, J.C. In, C.J. Min, W.C. Sun, H.S. Hyun, Morphology and physical properties of polyethylene/silicate nanocomposite prepared by melt intercalation, *J Polym Sci B Polym Phys*. 40 (2002) 1454–1463. <https://doi.org/10.1002/polb.10201>.
- [43] M. Yilmaz, A. Yilmaz, A. Karaman, F. Aysin, O. Aksakal, Monitoring chemically and green-synthesized silver nanoparticles in maize seedlings via surface-enhanced Raman spectroscopy (SERS) and their phytotoxicity evaluation, *Talanta*. 225 (2021). <https://doi.org/10.1016/j.talanta.2020.121952>.
- [44] A. Gök, S. Şen, Preparation and characterization of poly(2-chloroaniline)/SiO<sub>2</sub> nanocomposite via oxidative polymerization: Comparative UV-vis studies into different solvents of poly(2-chloroaniline) and poly(2-chloroaniline)/SiO<sub>2</sub>, *J Appl Polym Sci*. 102 (2006) 935–943. <https://doi.org/10.1002/app.24266>.
- [45] H. Boduğöz-Sentürk, O. Güven, Enhancement of conductivity in polyaniline-[poly(vinylidene chloride)-co-(vinyl acetate)] blends by irradiation, *Radiation Physics and Chemistry*. 80 (2011) 153–158. <https://doi.org/10.1016/j.radphyschem.2010.07.025>.
- [46] Y.-C. Liu, C.-J. Tsai, Characterization and enhancement in conductivity and conductivity stability of electropolymerized polypyrrole/Al<sub>2</sub>O<sub>3</sub> nanocomposites, n.d. [www.elsevier.com/locate/jelechem](http://www.elsevier.com/locate/jelechem).

- [47] X. Wang, S. Jiang, X. Huo, R. Xia, E. Muhire, M. Gao, Facile preparation of a TiO<sub>2</sub> quantum dot/graphitic carbon nitride heterojunction with highly efficient photocatalytic activity, *Nanotechnology*. 29 (2018). <https://doi.org/10.1088/1361-6528/aab1be>.
- [48] Z.G. Wu, Z.M. Ren, L. Li, L. Lv, Z. Chen, Hydrothermal synthesis of TiO<sub>2</sub> quantum dots with mixed titanium precursors, *Sep Purif Technol*. 251 (2020). <https://doi.org/10.1016/j.seppur.2020.117328>.
- [49] C. Uzun, P. Ilgin, O. Güven, Radiation induced in-situ generation of conductivity in the blends of polyaniline-base with chlorinated-polyisoprene, *Radiation Physics and Chemistry*. 79 (2010) 343–346. <https://doi.org/10.1016/j.radphyschem.2009.08.013>.
- [50] G. Vani, S. Jhancymary, Interfacial Polymerization and Characterization of Poly (2-Chloroaniline)-NiFe<sub>2</sub>O<sub>4</sub> Nanocomposite, (n.d.). [www.ijpbs.comorwww.ijpbsonline.com](http://www.ijpbs.comorwww.ijpbsonline.com).
- [51] L. Ghasemi-Mobarakeh, M.P. Prabhakaran, M. Morshed, M.H. Nasr-Esfahani, H. Baharvand, S. Kiani, S.S. Al-Deyab, S. Ramakrishna, Application of conductive polymers, scaffolds and electrical stimulation for nerve tissue engineering, *J Tissue Eng Regen Med*. 5 (2011). <https://doi.org/10.1002/term.383>.
- [52] P. Humpolicek, V. Kasparikova, P. Saha, J. Stejskal, Biocompatibility of polyaniline, *Synth Met*. 162 (2012) 722–727. <https://doi.org/10.1016/j.synthmet.2012.02.024>.
- [53] A. Hashemi Monfared, M. Jamshidi, Synthesis of polyaniline/titanium dioxide nanocomposite (PAni/TiO<sub>2</sub>) and its application as photocatalyst in acrylic pseudo paint for benzene removal under UV/VIS lights, *Prog Org Coat*. 136 (2019). <https://doi.org/10.1016/j.porgcoat.2019.105257>.
- [54] S.Y. Lee, S.J. Park, TiO<sub>2</sub> photocatalyst for water treatment applications, *Journal of Industrial and Engineering Chemistry*. 19 (2013) 1761–1769. <https://doi.org/10.1016/j.jiec.2013.07.012>.
- [55] R. Ameta, S. Benjamin, A. Ameta, S.C. Ameta, Photocatalytic degradation of organic pollutants: A review, *Materials Science Forum*. 734 (2013) 247–272. <https://doi.org/10.4028/www.scientific.net/MSF.734.247>.
- [56] A.E.H. Machado, A.M. Furuyama, S.Z. Falone, R. Ruggiero, D. Da Silva Perez, A. Castellan, Photocatalytic degradation of lignin and lignin models, using titanium dioxide: the role of the hydroxyl radical, n.d.
- [57] N.A. Jumat, P.S. Wai, J.J. Ching, W.J. Basirun, Synthesis of polyaniline-TiO<sub>2</sub> nanocomposites and their application in photocatalytic degradation, *Polymers and Polymer Composites*. 25 (2017) 507–514. <https://doi.org/10.1177/096739111702500701>.
- [58] K.M. Molapo, P.M. Ndagili, R.F. Ajayi, G. Mbambisa, S.M. Mailu, N. Njomo, M. Masikini, P. Baker, E.I. Iwuoha, *Electronics of Conjugated Polymers (I): Polyaniline*, 2012. [www.electrochemsci.org](http://www.electrochemsci.org).
- [59] A. Paleologou, H. Marakas, N.P. Xekoukoulotakis, A. Moya, Y. Vergara, N. Kalogerakis, P. Gikas, D. Mantzavinos, Disinfection of water and wastewater by TiO<sub>2</sub> photocatalysis, sonolysis and UV-C irradiation, *Catal Today*. 129 (2007) 136–142. <https://doi.org/10.1016/j.cattod.2007.06.059>.
- [60] S. Bagwasi, B. Tian, J. Zhang, M. Nasir, Synthesis, characterization and application of bismuth and boron Co-doped TiO<sub>2</sub>: A visible light active photocatalyst, *Chemical Engineering Journal*. 217 (2013) 108–118. <https://doi.org/10.1016/j.cej.2012.11.080>.
- [61] E.S.A.E. Ahmed, B.A. El-Sayed, W.A.A. Mohamed, A. Fahmy, A. Helal, Recycling of supported nanocomposites for hazardous industrial wastewater treatment via Solar photocatalytic process, *Egyptian Journal of Petroleum*. 30 (2021) 29–35. <https://doi.org/10.1016/j.ejpe.2021.02.001>.
- [62] W.A.A. Mohamed, H.A. Mousa, H.H. Abd El-Gawad, H.T. Handal, H.R. Galal, I.A. Ibrahim, S.D. Mekkey, M.A.M. Ahmed, S. Ben Mousa, A.A. Labib, Photophysical effects of TiO<sub>2</sub> quantum dots on phytotoxicity, recycling for solar and photocatalytic processes of industrial effluent, *Results Phys*. 46 (2023). <https://doi.org/10.1016/j.rinp.2023.106316>.
- [63] E.S.A.E. Ahmed, B.A. El-Sayed, W.A.A. Mohamed, A. Fahmy, A. Helal, Recycling of supported nanocomposites for hazardous industrial wastewater treatment via Solar photocatalytic process, *Egyptian Journal of Petroleum*. 30 (2021) 29–35. <https://doi.org/10.1016/j.ejpe.2021.02.001>.